An Implicit Method for Magnetic Fusion Extended MHD using Adaptive, High-Order, High-Continuity Finite Elements

S. C. Jardin, J. Breslau, N. Ferraro

Princeton Plasma Physics Laboratory

A. Bauer, M. Shephard

Rensselaer Polytechnic Institute

SIAM Annual Meeting

Boston, MA

July 13 2006

The Extended MHD equations for a magnetized (fusion) plasma are a high-order system of 8 scalar variables that are characterized by a wide range of space and timescales.

Our approach is as follows:

Multiple space scales	→	unstructured adaptive elements
Multiple time scales	→	implicit time differencing
High order derivatives	→	C^1 continuity elements (up to 4th order)
8 scalar variables	→	split implicit time advance & compact rep.
Strong magnetic field	→	stream function/potential representation

Extended MHD Equations:

Resistive MHD

2-fluid Extended MHD terms

$$\frac{\partial n}{\partial t} + \nabla \bullet (n\vec{V}) = 0$$

$$\frac{\partial \vec{B}}{\partial t} = -\nabla \times \vec{E} \qquad \vec{J} = \nabla \times \vec{B}$$

$$\vec{V} = \nabla U \times \hat{z} + \nabla_{\perp}\chi + V_z$$

$$\vec{B} = \nabla \psi \times \hat{z} + I\hat{z}$$

$$nM_i\left(\frac{\partial \vec{V}}{\partial t} + \vec{V} \bullet \nabla \vec{V}\right) + \nabla p = \vec{J} \times \vec{B} - \nabla \bullet \Pi_{GV} + \mu \nabla^2 \vec{V}$$

$$\vec{E} + \vec{V} \times \vec{B} = \eta \vec{J} + \frac{1}{ne}\left(\vec{J} \times \vec{B} - \nabla p_e\right) - \lambda_H (\Delta x)^2 \nabla^2 \vec{J}$$

$$\frac{3}{2}\frac{\partial p_e}{\partial t} + \nabla \bullet \left(\frac{3}{2} p_e \vec{V}\right) = -p_e \nabla \bullet \vec{V} + \eta J^2 + \frac{\vec{J}}{ne} \bullet \left[\frac{3}{2}\nabla p_e - \frac{5}{2}\frac{p_e}{n}\nabla n\right] - \nabla \bullet \vec{q}_e + Q_{\Delta}$$

$$\frac{3}{2}\frac{\partial p_i}{\partial t} + \nabla \bullet \left(\frac{3}{2} p_i \vec{V}\right) = -p_i \nabla \bullet \vec{V} + \mu \left|\nabla V\right|^2 - \nabla \bullet \vec{q}_i - Q_{\Delta}$$

8 scalar variables: $\psi, I, U, \chi, V_z, n, p_e, p_i$

Δx is typical zone (element) size

Scalar data is represented using 18 degree of freedom quintic triangular finite elements Q_{18}

- All data is at nodes: function + first 5 derivatives (6 dof)
- Complete quintic polynomial has 21 coefficients
    - 18 values come from the 3 nodes (3 x 6)
    - 3 values come from requirement that the normal derivative along each edge be only a (univariate) cubic….leads to C^1 continuity
- Contains a complete Taylor series through 4th order…error ~ h^5
- Compact representation … only 3 dof/triangle
- C^1 continuity allows up to 4th derivatives in space without introducing auxiliary variables
- Unstructured triangular mesh allows adaptive zoning

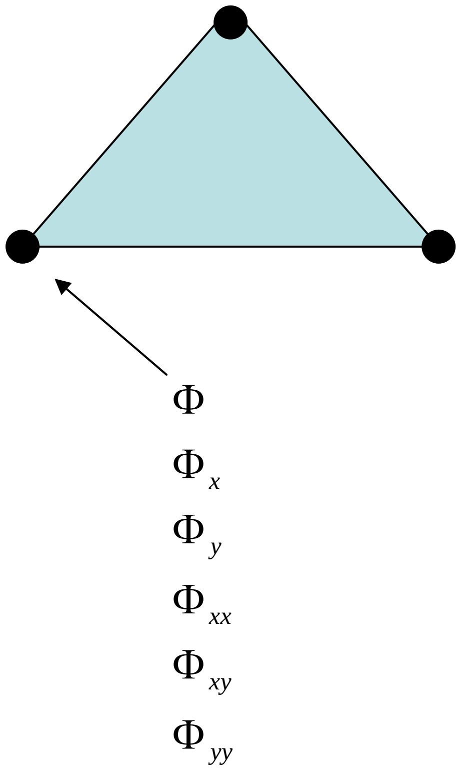

Implicit velocity time-advance substitutes in from field equations to contain all Ideal MHD wave phenomena

$$\rho\dot{\vec{V}} = \left(\vec{J} + \theta\delta t\dot{\vec{J}}\right)\times\left(\vec{B} + \theta\delta t\dot{\vec{B}}\right) - \nabla\left(P + \theta\delta t\dot{P}\right) + \cdots$$

$$\dot{\vec{J}} = \nabla\times\nabla\times\left[\left(\vec{V} + \theta\delta t\dot{\vec{V}}\right)\times B\right] + \cdots$$

$$\dot{\vec{B}} = \nabla\times\left[\left(\vec{V} + \theta\delta t\dot{\vec{V}}\right)\times B\right] + \cdots$$

$$\dot{P} = -\left(\vec{V} + \theta\delta t\dot{\vec{V}}\right)\bullet\nabla P - \frac{5}{3}P\nabla\bullet\left(\vec{V} + \theta\delta t\dot{\vec{V}}\right)$$

let $\dot{\vec{V}} = \dfrac{\vec{V}^{n+1} - \vec{V}^{n}}{\delta t}$, move all $\vec{V}^{n+1}$ terms to left side of equation

$$L_1\left\{V^{n+1}\right\} = L_2\left\{V^{n}\right\} + \cdots$$

Use SuperLU to invert this linear operator to get from time n to (n+1)

A similar technique is used on the magnetic field equations. Fully implicit Extended MHD (2-fluid) equations-- time step determined by accuracy only:

$$\begin{bmatrix} S_{11}^v & S_{12}^v & S_{13}^v \\ S_{21}^v & S_{22}^v & S_{23}^v \\ S_{31}^v & S_{32}^v & S_{33}^v \end{bmatrix} \bullet \begin{bmatrix} U \\ V_z \\ \chi \end{bmatrix}^{n+1} = \begin{bmatrix} D_{11}^v & D_{12}^v & D_{13}^v \\ D_{21}^v & D_{22}^v & D_{23}^v \\ D_{31}^v & D_{32}^v & D_{33}^v \end{bmatrix} \bullet \begin{bmatrix} U \\ V_z \\ \chi \end{bmatrix}^{n} + \begin{bmatrix} R_{11}^v & R_{12}^v & R_{13}^v \\ R_{21}^v & R_{22}^v & R_{23}^v \\ R_{31}^v & R_{32}^v & R_{33}^v \end{bmatrix} \bullet \begin{bmatrix} \psi \\ I \\ P_e \end{bmatrix}^{n}$$

$$\vec{V} = \nabla U \times \hat{z} + \nabla_\perp \chi + V_z$$
$$\vec{B} = \nabla \psi \times \hat{z} + I \hat{z}$$

Alfven Wave physics

$$S_{11}^n \bullet N^{n+1} = D_{11}^n \bullet N^n + \begin{bmatrix} R_{11}^n & R_{12}^n & R_{13}^n \end{bmatrix} \bullet \begin{bmatrix} U \\ V_z \\ \mathrm{X} \end{bmatrix}^{n+1} + \begin{bmatrix} Q_{11}^n & Q_{12}^n & Q_{13}^n \end{bmatrix} \bullet \begin{bmatrix} U \\ V_z \\ \mathrm{X} \end{bmatrix}^{n} + Q_{14}^n$$

density

$$S_{11}^p \bullet P^{n+1} = D_{11}^p \bullet P^n + \begin{bmatrix} R_{11}^p & R_{12}^p & R_{13}^p \end{bmatrix} \bullet \begin{bmatrix} U \\ V_z \\ \mathrm{X} \end{bmatrix}^{n+1} + \begin{bmatrix} Q_{11}^p & Q_{12}^p & Q_{13}^p \end{bmatrix} \bullet \begin{bmatrix} U \\ V_z \\ \mathrm{X} \end{bmatrix}^{n} + Q_{14}^p$$

pressure

$$\begin{bmatrix} S_{11}^p & S_{12}^p & S_{13}^p \\ S_{21}^p & S_{22}^p & S_{23}^p \\ S_{31}^p & S_{32}^p & S_{33}^p \end{bmatrix} \bullet \begin{bmatrix} \psi \\ I \\ P_e \end{bmatrix}^{n+1} = \begin{bmatrix} D_{11}^p & D_{12}^p & D_{13}^p \\ D_{21}^p & D_{22}^p & D_{23}^p \\ D_{31}^p & D_{32}^p & D_{33}^p \end{bmatrix} \bullet \begin{bmatrix} \psi \\ I \\ P_e \end{bmatrix}^{n} + \begin{bmatrix} R_{11}^p & R_{12}^p & R_{13}^p \\ R_{21}^p & R_{22}^p & R_{23}^p \\ R_{31}^p & R_{32}^p & R_{33}^p \end{bmatrix} \bullet \begin{bmatrix} U \\ V_z \\ \chi \end{bmatrix}^{n+1} + \begin{bmatrix} Q_{11}^p & Q_{12}^p & Q_{13}^p \\ Q_{21}^p & Q_{22}^p & Q_{23}^p \\ Q_{31}^p & Q_{32}^p & Q_{33}^p \end{bmatrix} \bullet \begin{bmatrix} U \\ V_z \\ \chi \end{bmatrix}^{n}$$

Whistler, KAW, field diffusion physics

- 4 sequential matrix solves per time step
- 3 non-trivial subsets with 6,4,2 variables

GEM Nonlinear Benchmark

Poloidal Flux Ψ

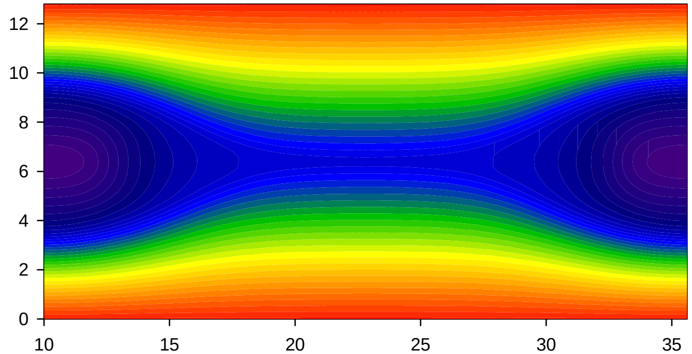

Current Density J

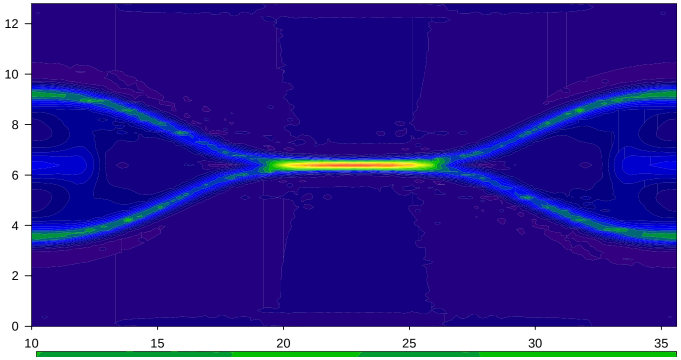

GEM Reconnection Problem

$$\psi^0(x,y) = \frac{1}{2}\ln(\cosh 2y)$$

$$P^0(x,y) = \left[\operatorname{sec}h^2 2y + 0.2\right]$$

$$\tilde{\psi}(x,y) = \varepsilon \cos k_x x \cos k_y y$$

1. Resistive MHD
   High and Low Viscosity
   ($\mu = 10\ \eta$, $\mu = 0.1\ \eta$)
2. Two-Fluid

- Provides a non-trivial, convenient test problem for code verification and validation and cross-code comparison
- Also, extending this by adding an equilibrium magnetic field into the plane (guide field)

Resistive MHD gives convergent results. Time step depends on accuracy requirement only

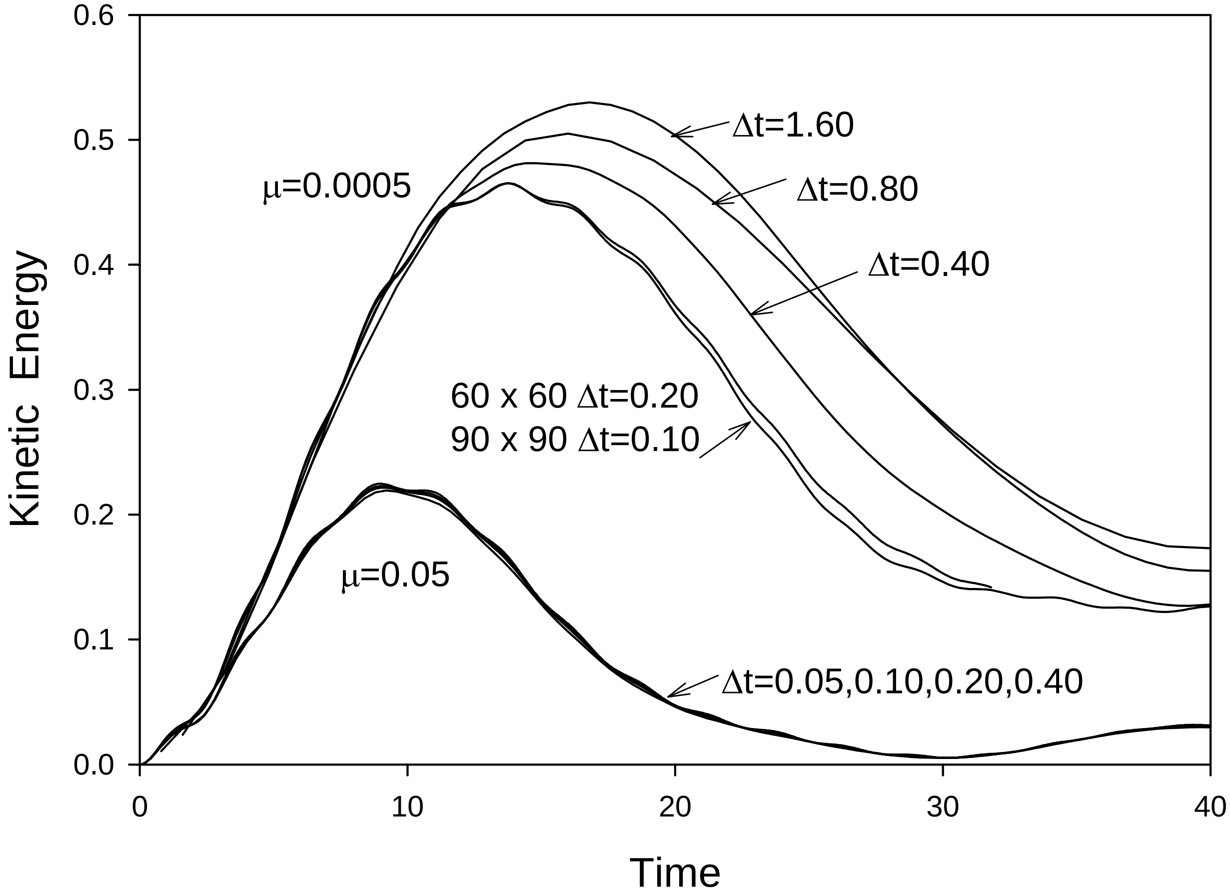

- Dependence of kinetic energy on viscosity (varies by 100)
- Lower viscosity cases require smaller timestep for accuracy
- 60 x 60 grid gives adequate spatial resolution

Current Density contours for resistive MHD case

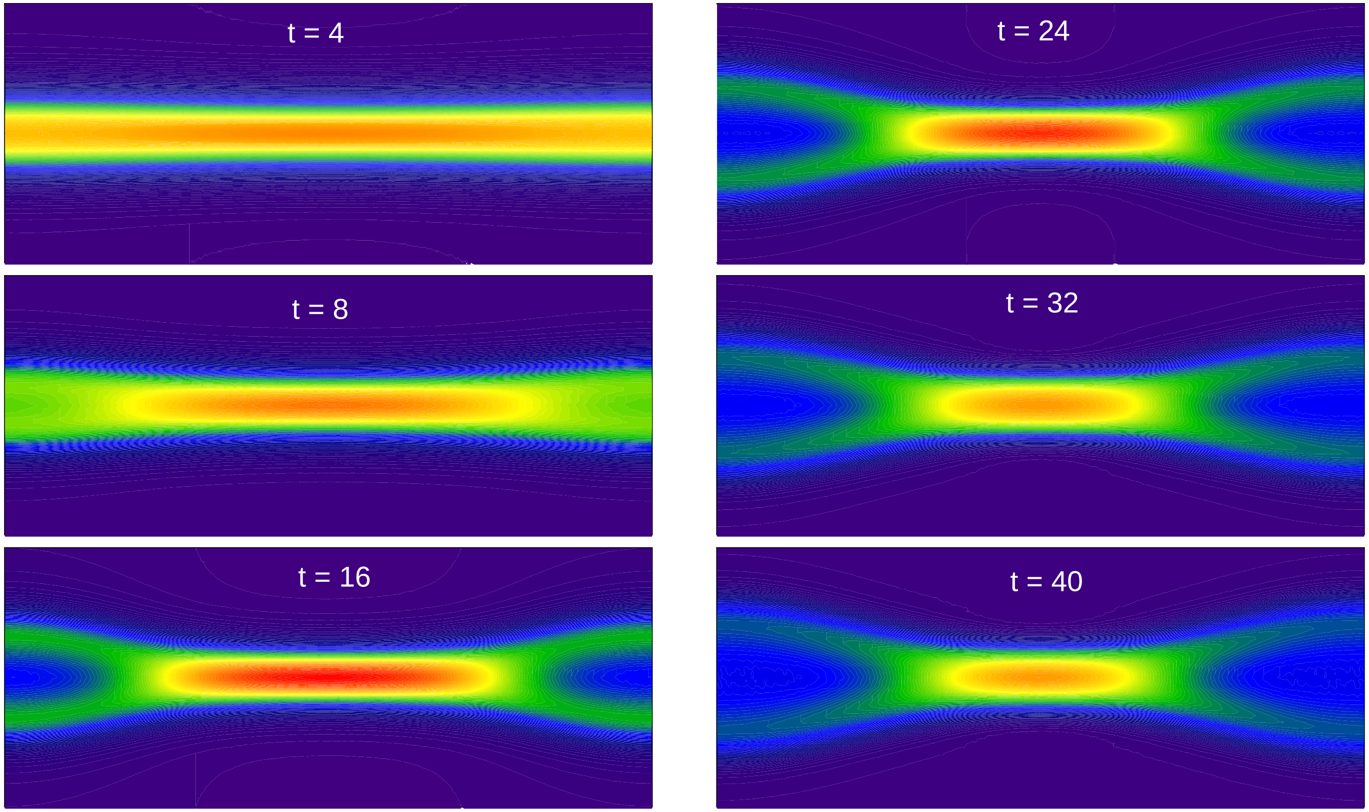

Resolution requirements are modest for resistive MHD; $\eta = .005$, $\nu=10\eta$

2-fluid reconnection qualitatively different, requires high resolution for convergent results

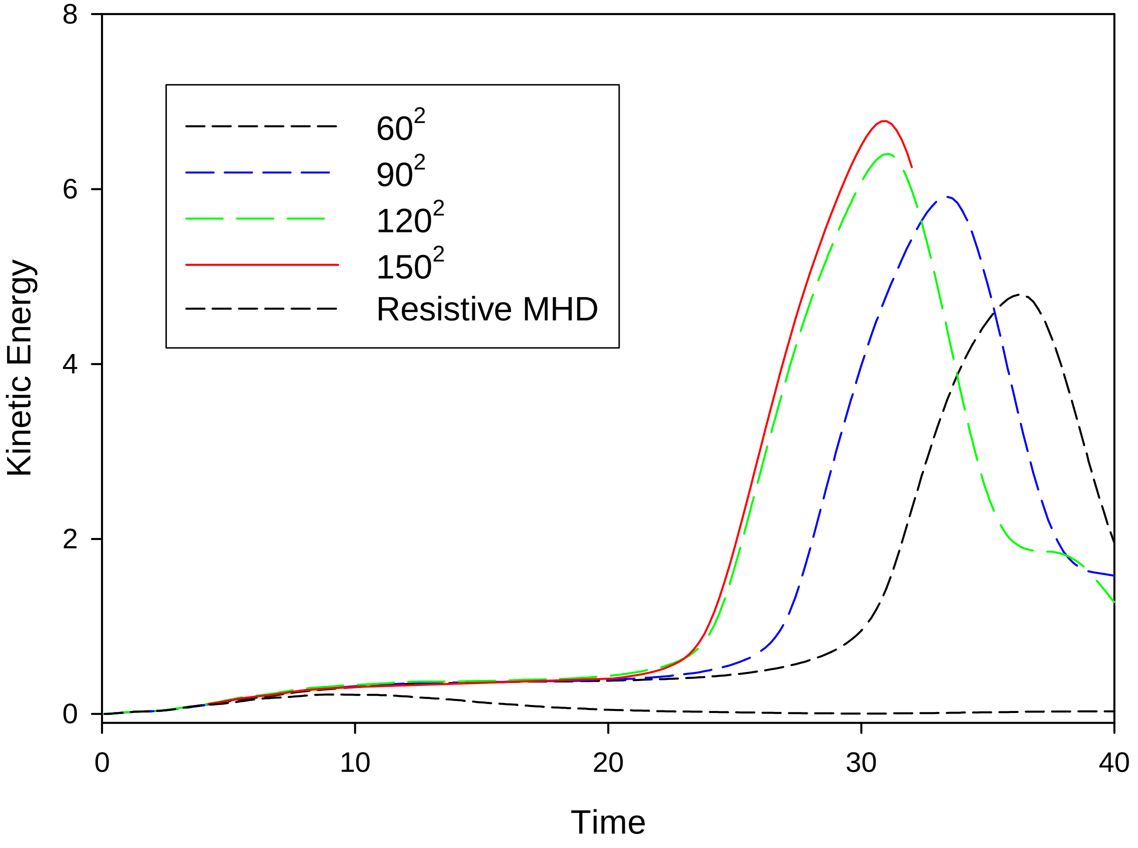

- Note sudden transition where velocity abruptly increases

- These calculations used a hyperviscosity term in Ohm's law proportional to $(\Delta x)^2 \cdots$ required for a stable calculation

Current Density contours for 2-fluid MHD

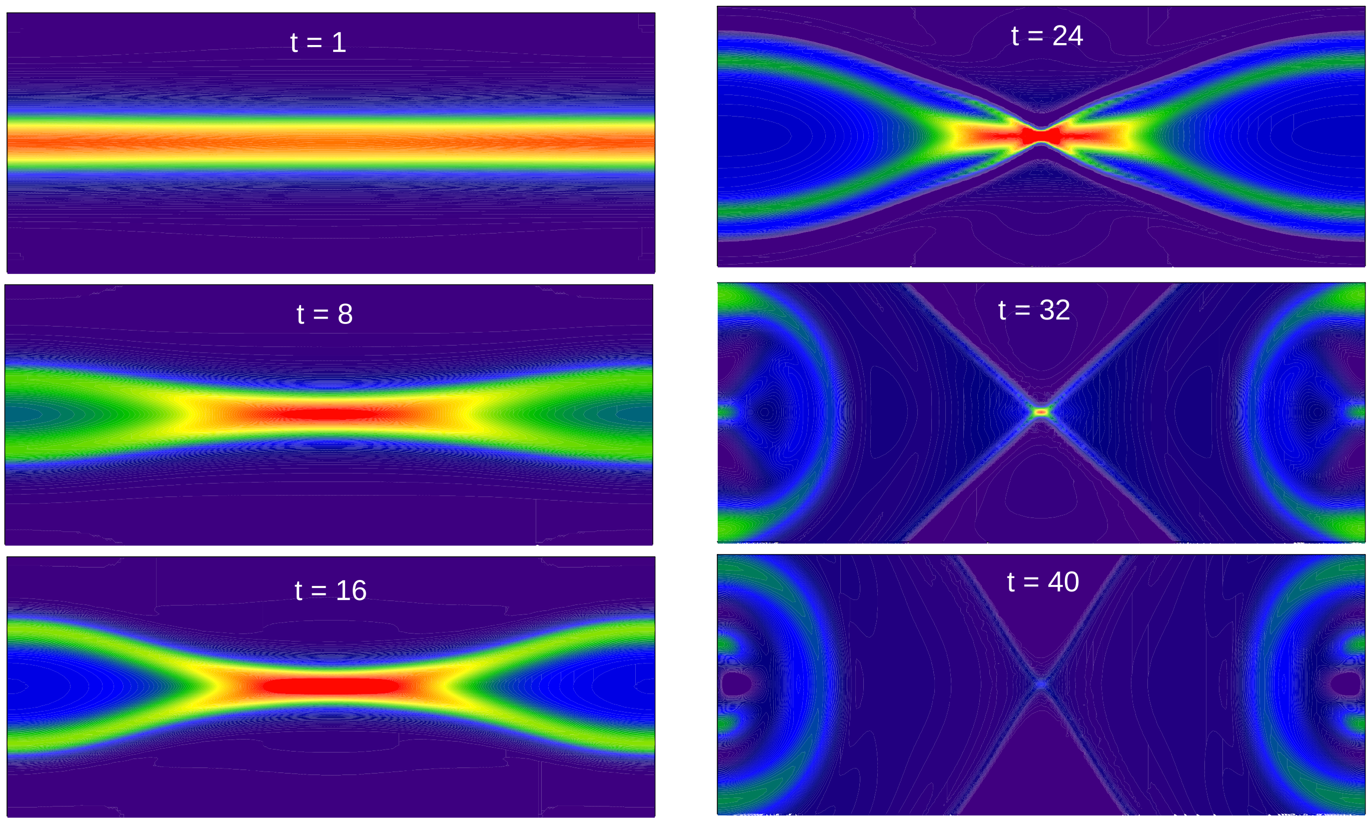

- Starts like resistive MHD
- Dramatic change in configuration for t > 20

Close-up of 2-fluid current density at t=32

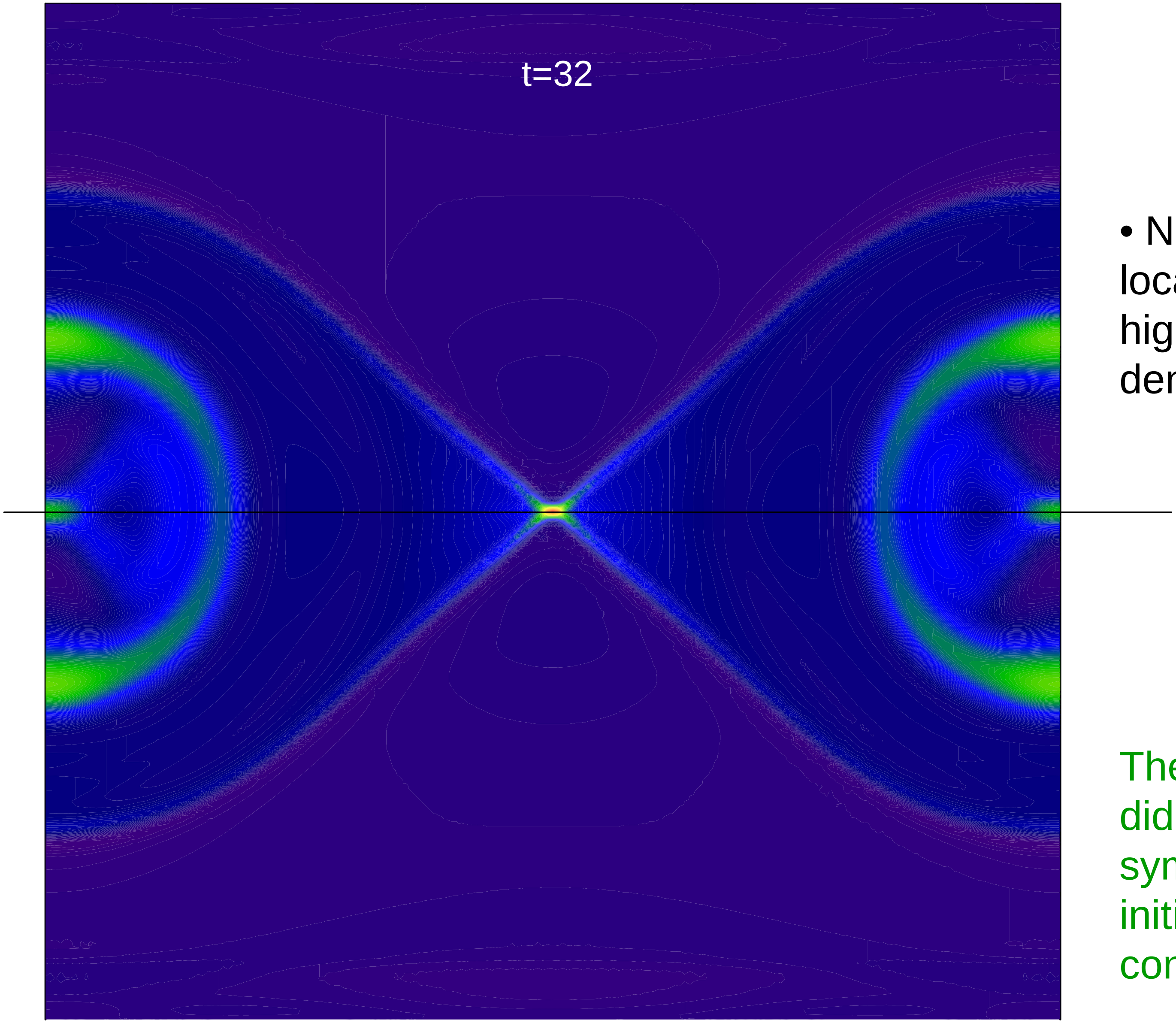

midplane

• Note very localized region of high current density in center

These calculations did not assume any symmetry, except for initial and boundary conditions

Midplane Current density collapses to the width of 1-3 triangular elements

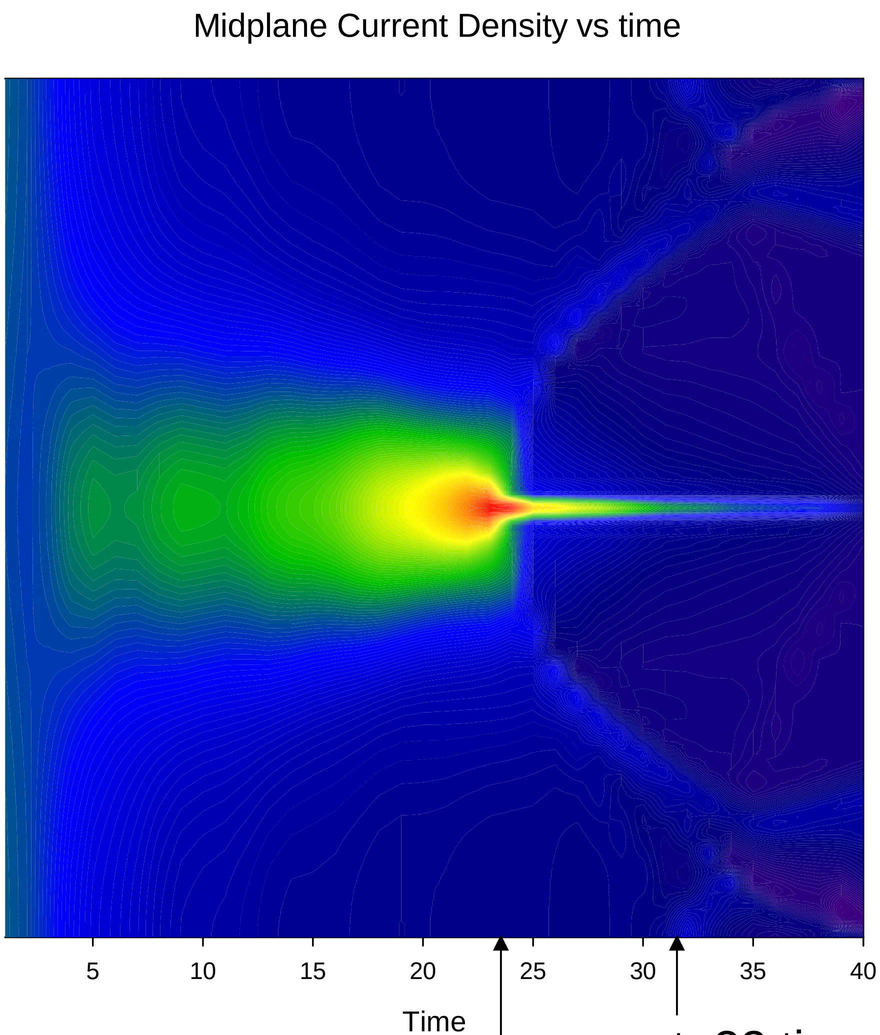

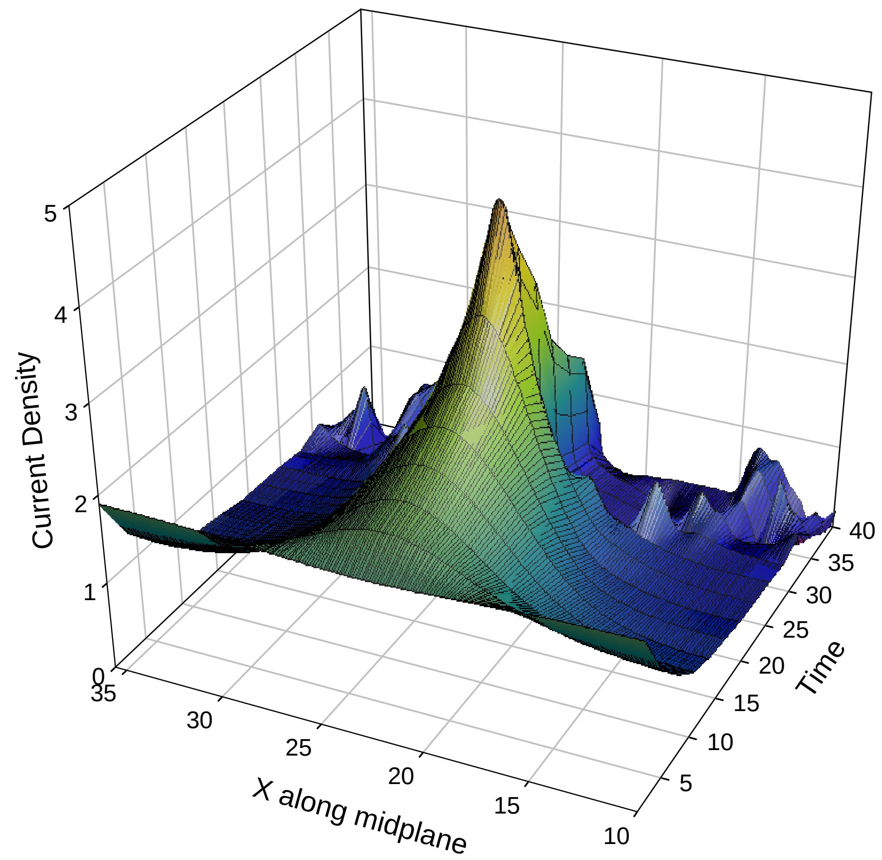

t=32 time of previous contour plot

(note sudden collapse at t=24)

Reconnection rate and maximum velocity for resistive and 2-fluid cases

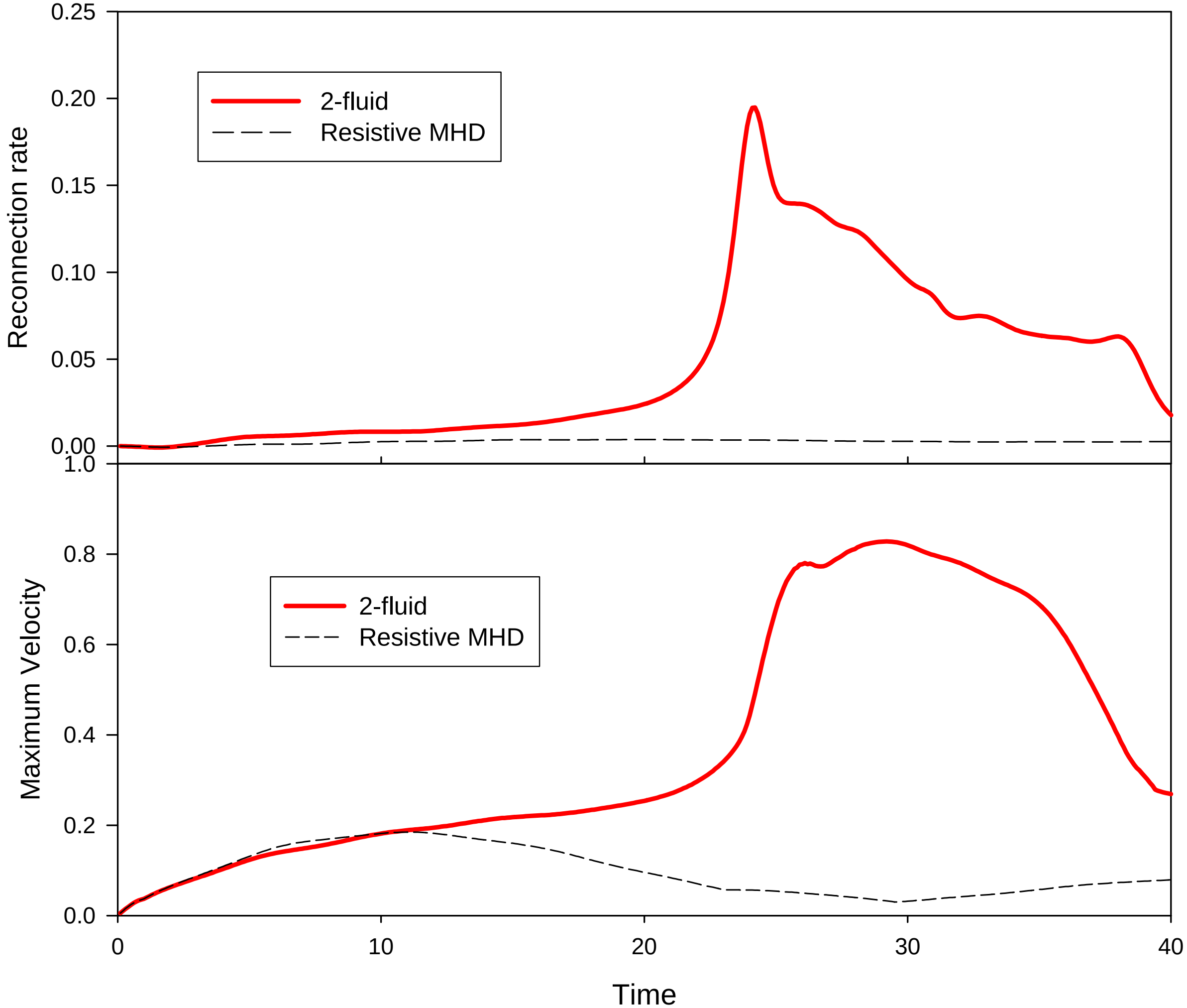

- note transition at t ~ 24 for 2-fluid case
- After transition, 2-fluid reconnection rate is over 50 times larger than resistive MHD rate

Midplane electric field before and after transition

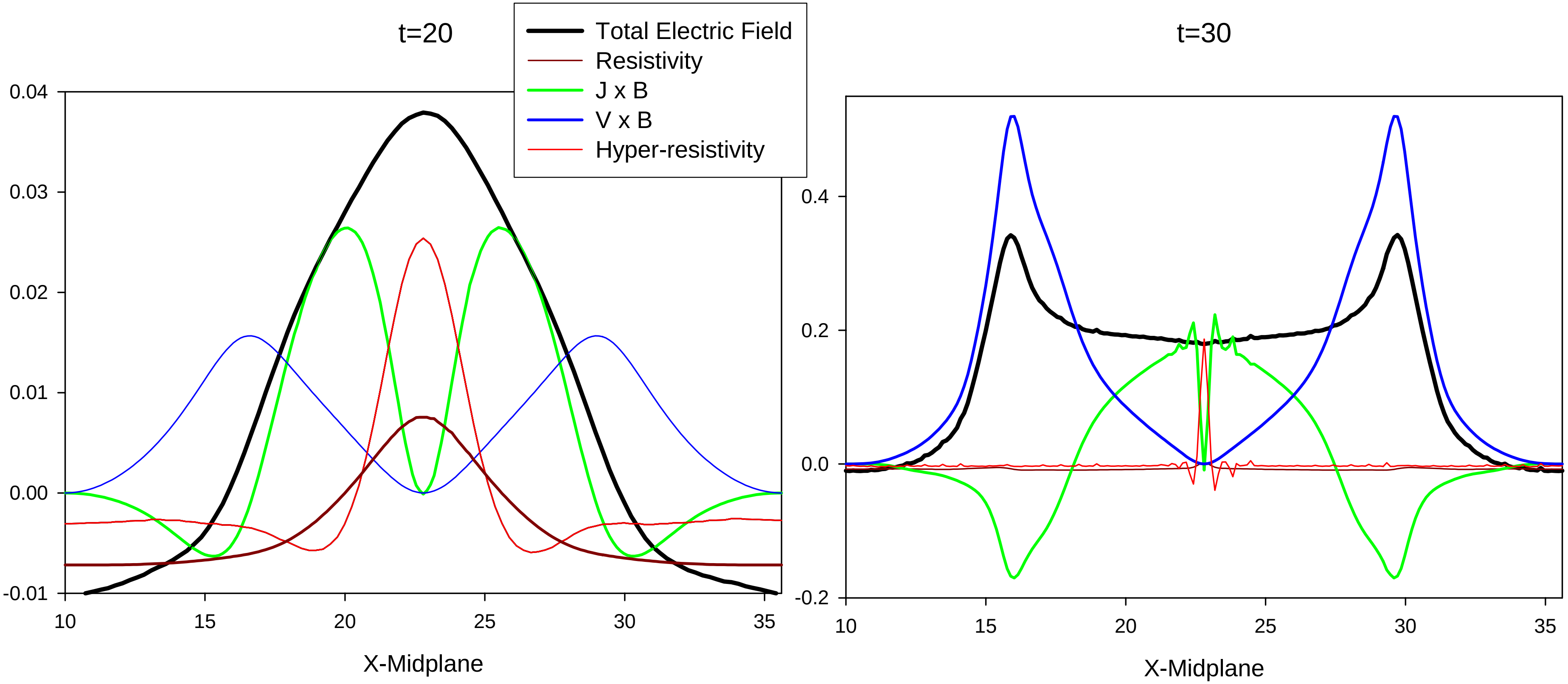

Reconnection rate: $$\hat{z}\bullet\left[\vec{E} = -\vec{V}\times\vec{B} + \eta\vec{J} + \frac{1}{ne}\left(\vec{J}\times\vec{B} - \nabla p_e\right) - \lambda_H(\Delta x)^2\nabla^2\vec{J}\right]$$

Midplane electric field before and after transition

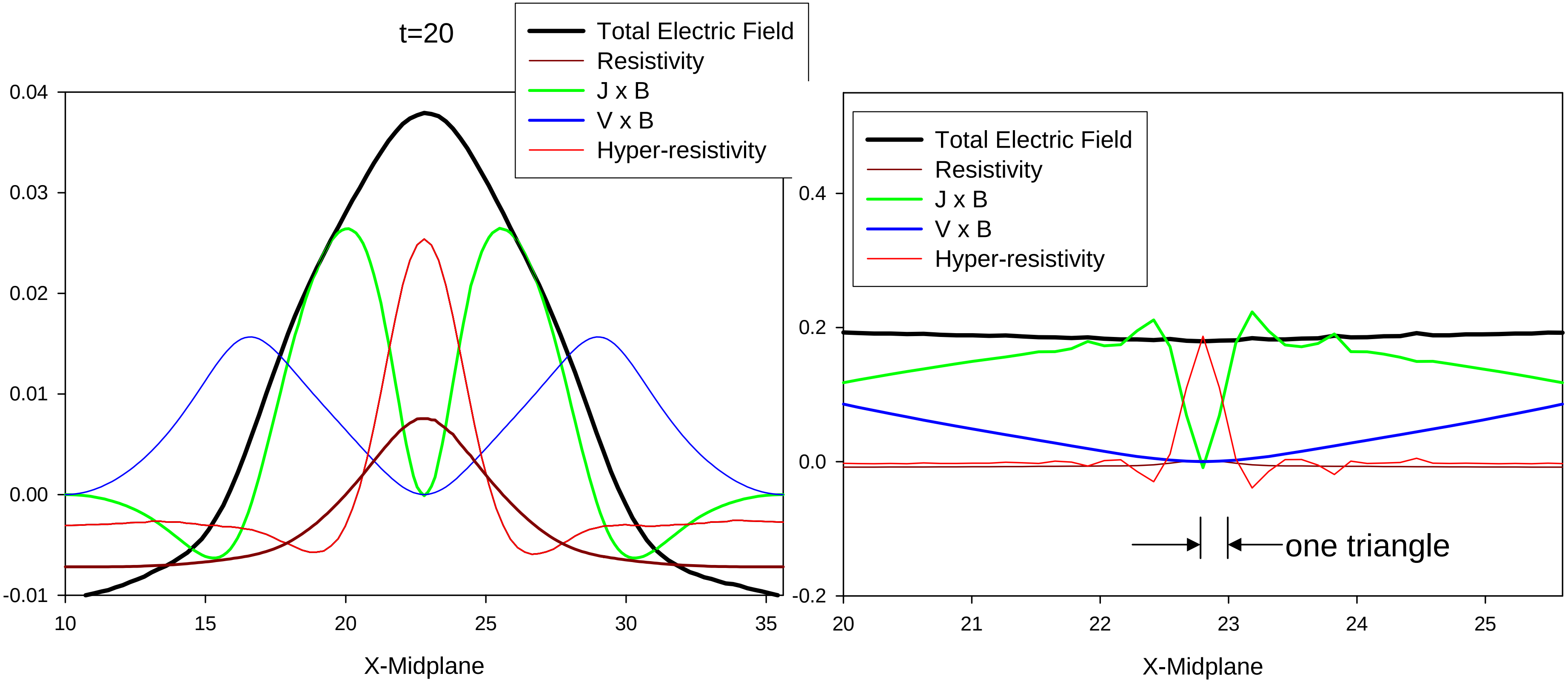

$$\hat{z}\bullet\left[\vec{E} = -\vec{V}\times\vec{B} + \eta\vec{J} + \frac{1}{ne}\left(\vec{J}\times\vec{B} - \nabla p_e\right) - \lambda_H (\Delta x)^2 \nabla^2 \vec{J}\right]$$

Hyper-resistivity coefficient must be large enough that current density collapse is limited to 1-2 triangles: *reason for factor $(\Delta x)^2$*

Test of sensitivity to hyperresistivity coefficient λ_H

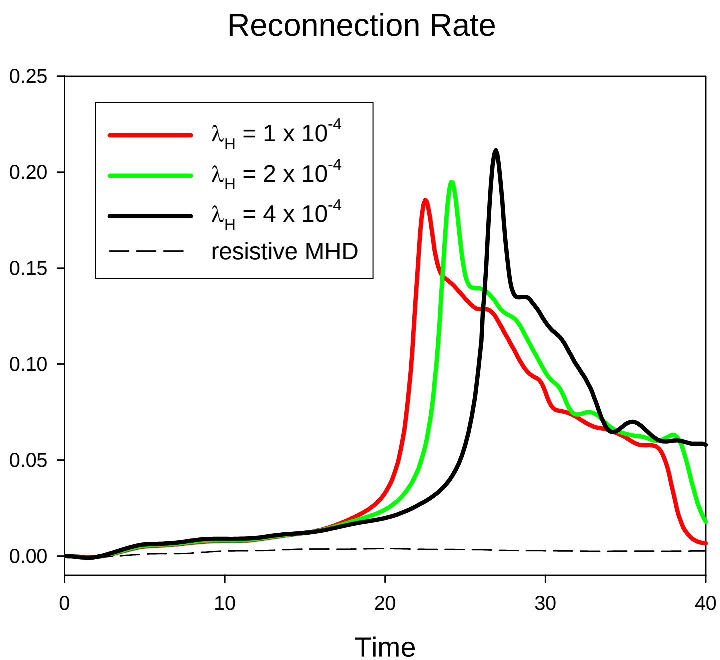

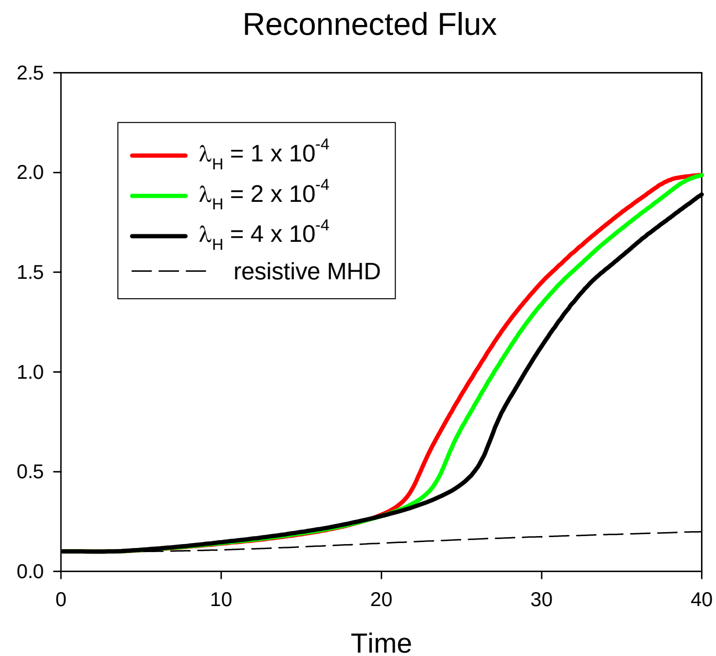

- These calculations had $(120)^2$ grid, everything else fixed
- In caption is value of of $\lambda_H(\Delta x)^2$
- Appears to be converging to a unique answer for $\lambda_H (\Delta x)^2 \rightarrow 0$
- Need for small value of $\lambda_H (\Delta x)^2$ implies need for small Δx (to avoid current layer collapsing to less than one zone width)

Effect of adding a guide field on 2-fluid reconnection

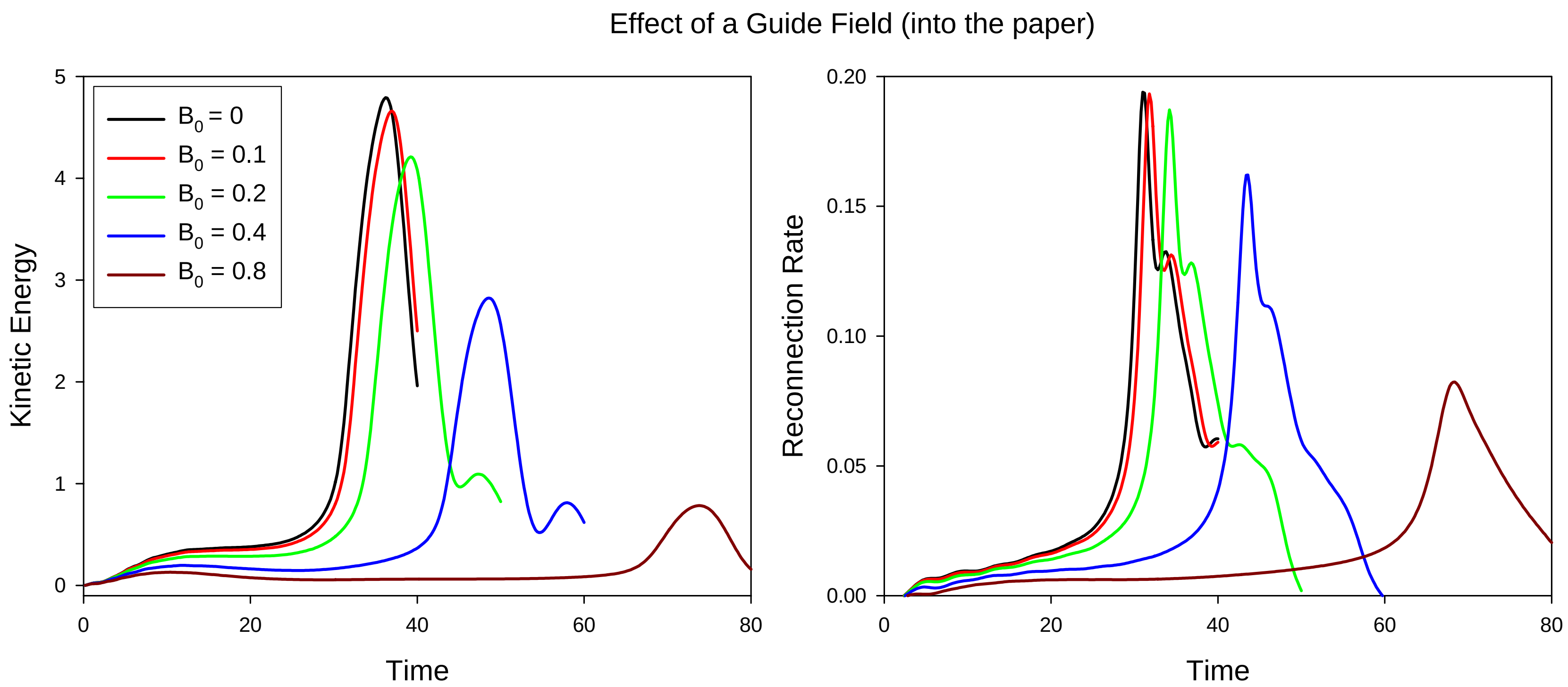

- Adding a guide field delays transition time and reduces maximum reconnection rate
- Small effect for $B_0 < 0.2$
- To be studied further

Change in velocity field with toroidal field strength

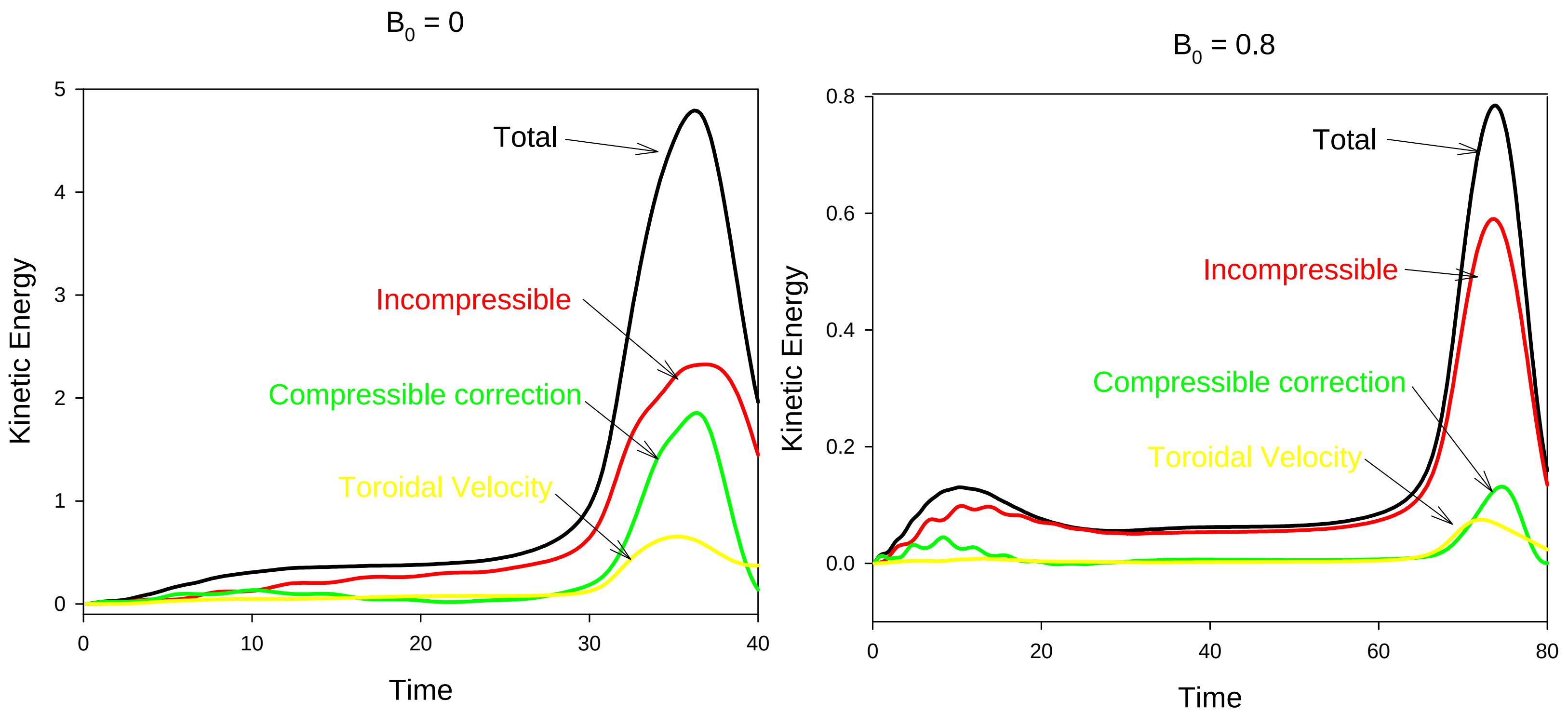

- Velocity field becomes more like incompressible flow as toroidal field strength increases

Adaptive Meshing

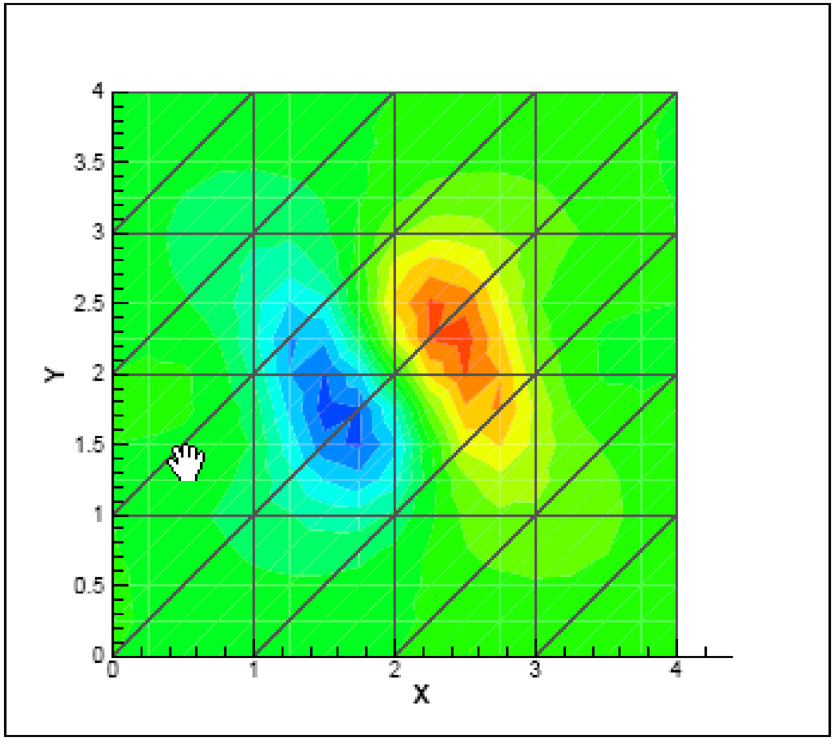

(a) Initial mesh

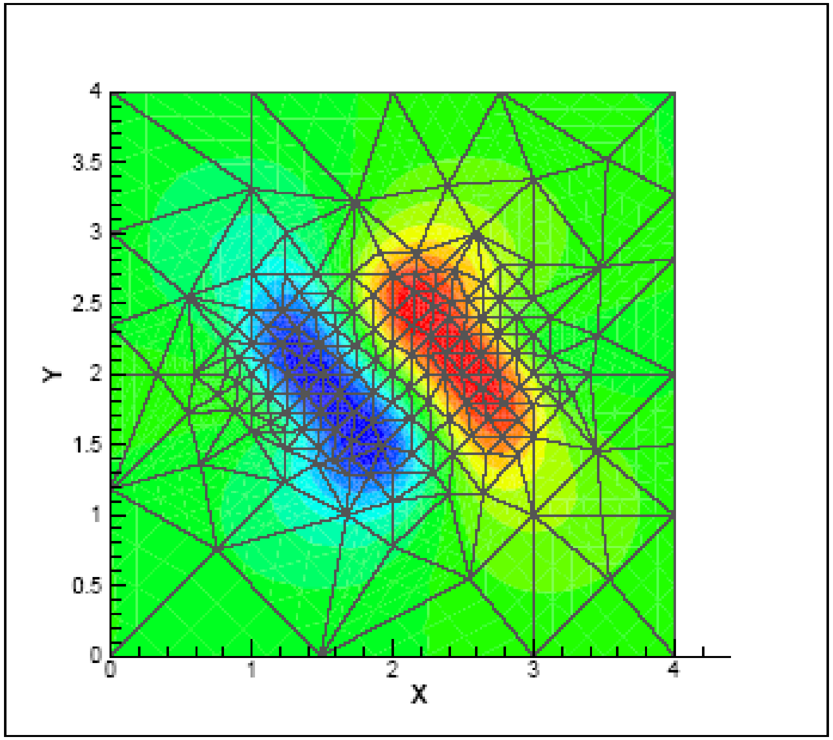

(b) Adapted mesh

Andy Bauer (RPI) has implemented an arbitrary Adapted Mesh in the M3D-C^1 code and is exploring different adaptive strategies. This should greatly improve the efficiency of the 2-fluid reconnection problem.

Summary and Conclusions

- Full 8-field E-MHD equations solved in 2D slab geometry with stream function/potential form
- Q_{18} elements allow high accuracy, compact representation of solution
- Implicit solution technique implies time step can be set by accuracy requirements, not stability
- 2-fluid reconnection problems require localized regions with high resolution…natural for adaptive refinement
- Extensions to toroidal geometry and 3D underway

Supplementary vgs if time permits

Tests of the 2-fluid and Gyroviscous terms: Gravitational Instability

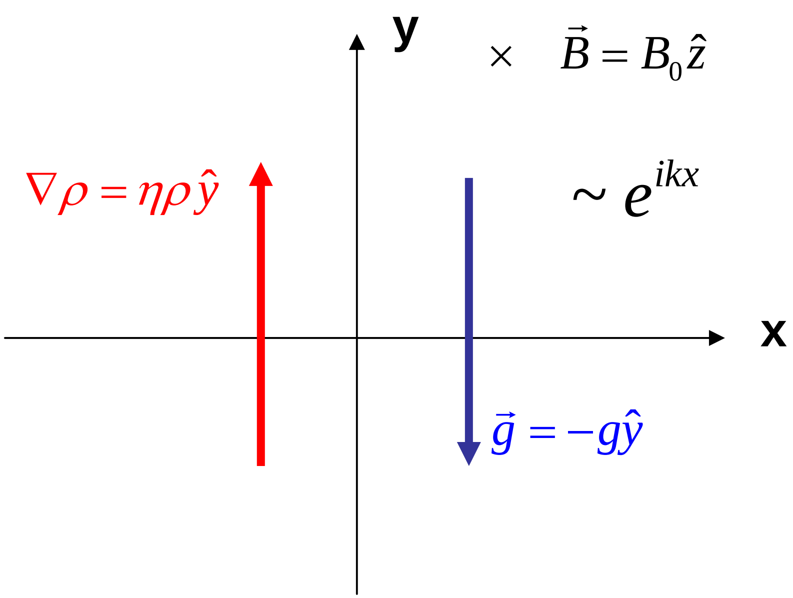

$$\frac{\partial \rho}{\partial t} + \nabla \bullet (\rho \vec{V}) = 0 \qquad p = p_i(\rho)$$

$$\frac{\partial \vec{B}}{\partial t} = \nabla \times \left[\vec{V} \times \vec{B} - \frac{1}{ne}\left(\vec{J} \times \vec{B} \right) \right] \qquad \vec{J} = \nabla \times \vec{B}$$

$$nM_i\left(\frac{\partial \vec{V}}{\partial t} + \vec{V} \bullet \nabla \vec{V}\right) + \nabla p = \vec{J} \times \vec{B} - \nabla \bullet \Pi_{GV}$$

Low-β result (R&T)

$$\omega^2 - \omega_* \omega + \gamma_{MHD}^2 = 0$$

$$\omega_* = \omega_{*2F} + \omega_{*GV}, \quad \gamma_{MHD}^2 = \frac{g}{L}$$

$$\omega_{*2F} = \frac{gk}{\Omega}, \quad \omega_{*GV} = \frac{1}{2}\frac{\rho_i^2 k^2}{kL}\Omega$$

$$\omega = \frac{1}{2}\left(\omega_* \pm \sqrt{\omega_*^2 - 4\gamma_{MHD}^2} \right)$$

Stable if: $\omega_* > 2\gamma_{MHD}$

Braginskii gyro-viscosity in M3D-C^1:

$$\nabla\cdot\overleftrightarrow{\Pi}=\left\{\left[\nabla\times\left(\frac{mp}{eB^2}\vec{B}\right)\right]\cdot\nabla\right\}\vec{V}-\nabla\left[\frac{mp}{2eB^2}\vec{B}\cdot\left(\nabla\times\vec{V}\right)\right]-\nabla\times\left\{\frac{mp}{eB^2}\left[(B\cdot\nabla)\vec{V}+\frac{1}{2}\left(\nabla\cdot\vec{V}-\frac{3}{B^2}\vec{B}\cdot\left[\left(\vec{B}\cdot\nabla\right)\vec{V}\right]\right)\vec{B}\right]\right\}$$
$$+(B\cdot\nabla)\left\{\frac{mp}{eB^2}\left(\frac{3}{B^2}\vec{B}\times\left[\left(\vec{B}\cdot\nabla\right)\vec{V}\right]+\frac{3}{2B^2}\left[\vec{B}\cdot\left(\nabla\times\vec{V}\right)\right]\vec{B}-\nabla\times\vec{V}\right)\right\}$$

Ramos

$$\hat{z}\cdot\quad\rightarrow\quad[V_z,\alpha I]-\alpha\left\{\left[\psi,\nabla_\perp^2U\right]+\left[\frac{\partial\psi}{\partial x},\frac{\partial U}{\partial x}-\frac{\partial\chi}{\partial y}\right]+\left[\frac{\partial\psi}{\partial y},\frac{\partial U}{\partial y}+\frac{\partial\chi}{\partial x}\right]\right\}-\frac{\partial\alpha}{\partial x}\left[\psi,\frac{\partial U}{\partial x}-\frac{\partial\chi}{\partial y}\right]-\frac{\partial\alpha}{\partial y}\left[\psi,\frac{\partial U}{\partial y}+\frac{\partial\chi}{\partial x}\right]$$
$$+\frac{1}{2}\alpha\nabla_\perp^2\chi\nabla_\perp^2\psi+\frac{1}{2}\left(\alpha\nabla_\perp^2\chi,\psi\right)-\frac{1}{2}\left[(\gamma\kappa,\psi)+\gamma\kappa\nabla_\perp^2\psi\right]+[\gamma\xi_z,\psi]+\frac{1}{2}[\lambda I,\psi]+\left[\alpha\nabla_\perp^2U,\psi\right]$$

$$-\hat{z}\cdot\nabla\times\quad\rightarrow\quad\left[\frac{\partial\chi}{\partial x}+\frac{\partial U}{\partial y},\frac{\partial(\alpha I)}{\partial y}\right]-\left[\frac{\partial\chi}{\partial y}-\frac{\partial U}{\partial x},\frac{\partial(\alpha I)}{\partial x}\right]+\left[\nabla_\perp^2U,\alpha I\right]+\nabla_\perp^2\left\{\alpha[\psi,V_z]\right\}-\frac{1}{2}\nabla_\perp^2\left(\alpha I\nabla_\perp^2\chi\right)+\frac{1}{2}\nabla_\perp^2(\gamma\kappa I)$$
$$+\frac{\partial}{\partial y}[\gamma\xi_x,\psi]-\frac{\partial}{\partial x}[\gamma\xi_y,\psi]+\frac{1}{2}\left\{\frac{\partial\lambda}{\partial x}\left[\frac{\partial\psi}{\partial x},\psi\right]+\frac{\partial\lambda}{\partial y}\left[\frac{\partial\psi}{\partial y},\psi\right]+([\lambda,\psi],\psi)+\left[\lambda\nabla_\perp^2\psi,\psi\right]\right\}+\frac{\partial}{\partial x}\left[\psi,\alpha\frac{\partial V_z}{\partial x}\right]+\frac{\partial}{\partial y}\left[\psi,\alpha\frac{\partial V_z}{\partial y}\right]$$

$$\nabla\cdot\quad\rightarrow\quad\left[\frac{\partial\chi}{\partial x}+\frac{\partial U}{\partial y},\frac{\partial(\alpha I)}{\partial x}\right]+\left[\frac{\partial\chi}{\partial y}-\frac{\partial U}{\partial x},\frac{\partial(\alpha I)}{\partial y}\right]+\left[\nabla_\perp^2\chi,\alpha I\right]+\frac{1}{2}\nabla_\perp^2\left\{\alpha\left[I\nabla_\perp^2U-(\psi,V_z)\right]\right\}+\frac{\partial}{\partial x}[\gamma\xi_x,\psi]+\frac{\partial}{\partial y}[\gamma\xi_y,\psi]$$
$$+\frac{1}{2}[[\lambda,\psi],\psi]+\lambda\left[\frac{\partial\psi}{\partial y},\frac{\partial\psi}{\partial x}\right]+\frac{1}{2}\frac{\partial\lambda}{\partial x}\left[\frac{\partial\psi}{\partial y},\psi\right]-\frac{1}{2}\frac{\partial\lambda}{\partial y}\left[\frac{\partial\psi}{\partial x},\psi\right]+\frac{\partial}{\partial x}\left\{\alpha\left[\psi,\frac{\partial V_z}{\partial y}\right]\right\}-\frac{\partial}{\partial y}\left\{\alpha\left[\psi,\frac{\partial V_z}{\partial x}\right]\right\}+[V_z,[\alpha,\psi]]$$

$$\alpha\equiv\frac{ep}{mB^2}=\frac{ep/m}{\left(\frac{\partial\psi}{\partial x}\right)^2+\left(\frac{\partial\psi}{\partial y}\right)^2+I^2}\qquad\gamma=\frac{3ep/m}{\left[\left(\frac{\partial\psi}{\partial x}\right)^2+\left(\frac{\partial\psi}{\partial y}\right)^2+I^2\right]^2}$$

$$\vec{\xi}=\left\{\frac{\partial\psi}{\partial x}[\psi,V_z]+I\left[\psi,\frac{\partial\chi}{\partial y}-\frac{\partial U}{\partial x}\right]\right\}\hat{x}+\left\{\frac{\partial\psi}{\partial y}[\psi,V_z]-I\left[\psi,\frac{\partial\chi}{\partial x}+\frac{\partial U}{\partial y}\right]\right\}\hat{y}-\left\{\frac{\partial\psi}{\partial x}\left[\psi,\frac{\partial\chi}{\partial x}+\frac{\partial U}{\partial y}\right]+\frac{\partial\psi}{\partial y}\left[\psi,\frac{\partial\chi}{\partial y}-\frac{\partial U}{\partial x}\right]\right\}\hat{z}$$

$$\lambda=\gamma\left[(\psi,V_z)-I\nabla_\perp^2U\right]$$

$$\kappa\equiv\frac{\partial\psi}{\partial y}\left[\frac{\partial\chi}{\partial x}+\frac{\partial U}{\partial y},\psi\right]-\frac{\partial\psi}{\partial x}\left[\frac{\partial\chi}{\partial y}-\frac{\partial U}{\partial x},\psi\right]+I[V_z,\psi]$$

Breslau

M3D-C^1 Gravitational Instability stabilized by Gyroviscosity

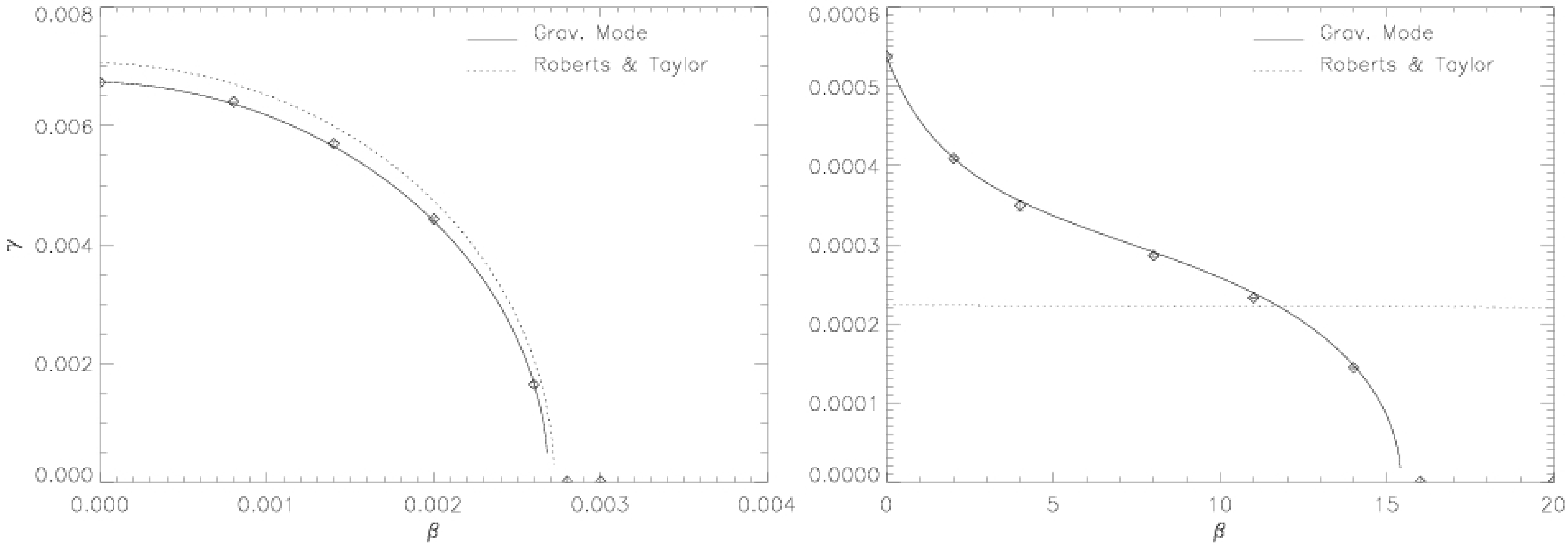

We have calculated the stabilization of the gravitational instability by Gyroviscosity: low beta (left) and high beta (right)

Ferraro

M3D-C^1…Gravitational Instability: nonlinear

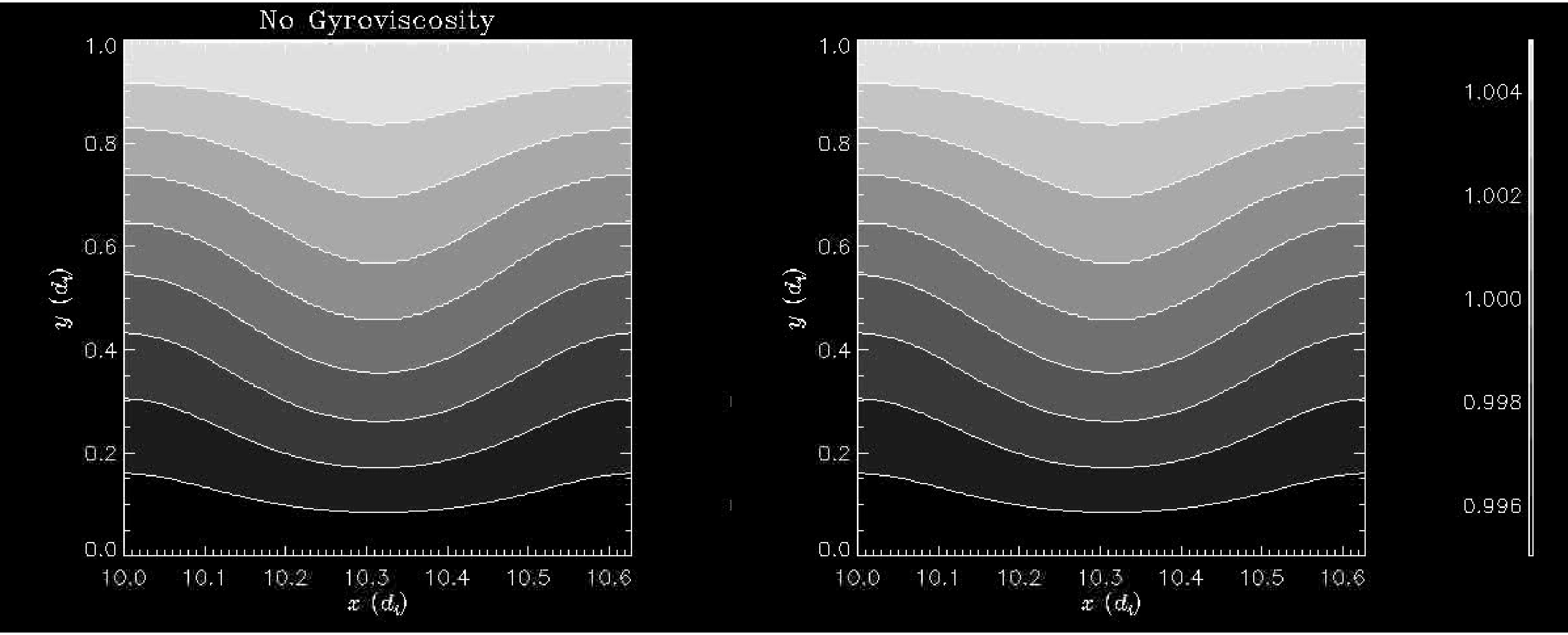

Ferraro

Anisotropic Diffusion

Shows greater than N^{-5} convergence

$$\frac{\partial T}{\partial t} = \nabla \bullet \left[\kappa_{\|} \frac{\vec{B}\vec{B}}{B^2} \bullet \nabla T \right] + \nabla^2 T + S$$

Solve to steady state

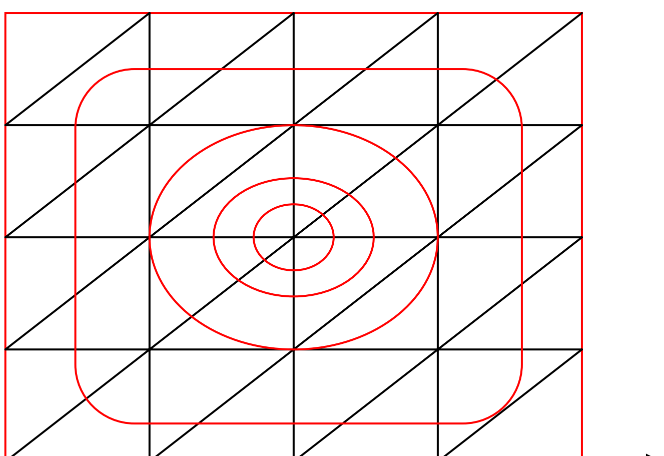

$$S = \psi = \cos\frac{\pi x}{L} \cos\frac{\pi y}{L}$$

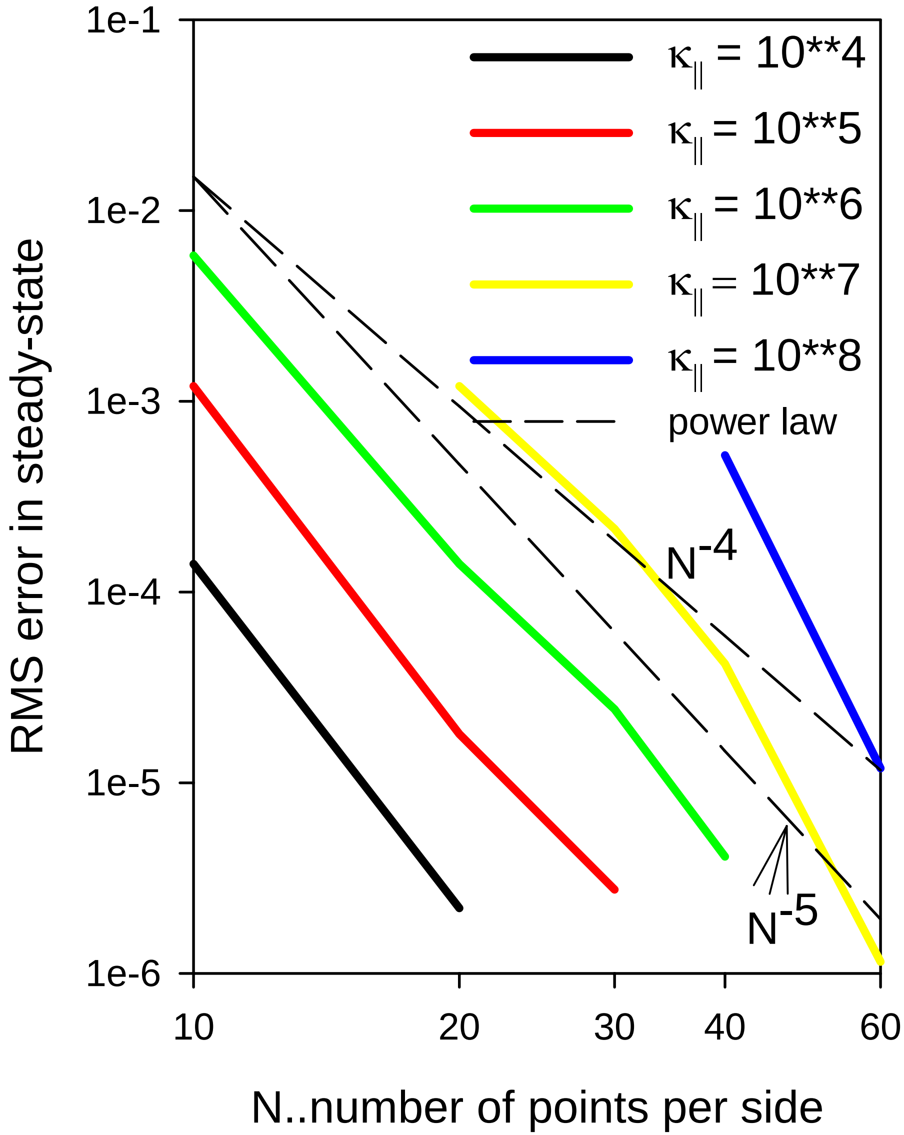

Non-linear evolution of tilting cylinder in full 6-field 2-fluid model

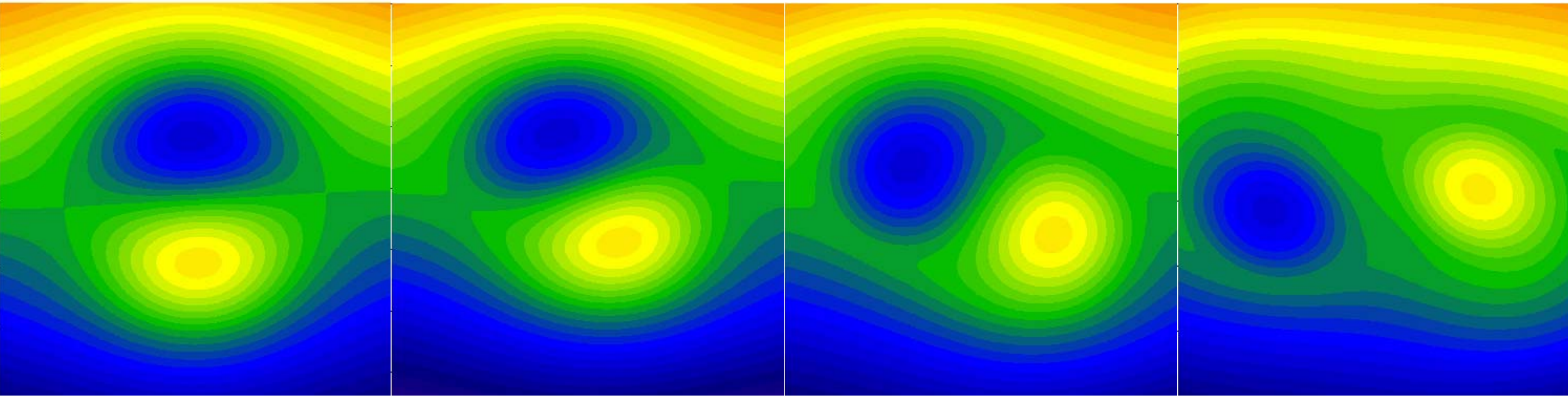

Ψ: t=0.8 | Ψ: t=3.8 | Ψ: t=4.0 | Ψ: t=4.8

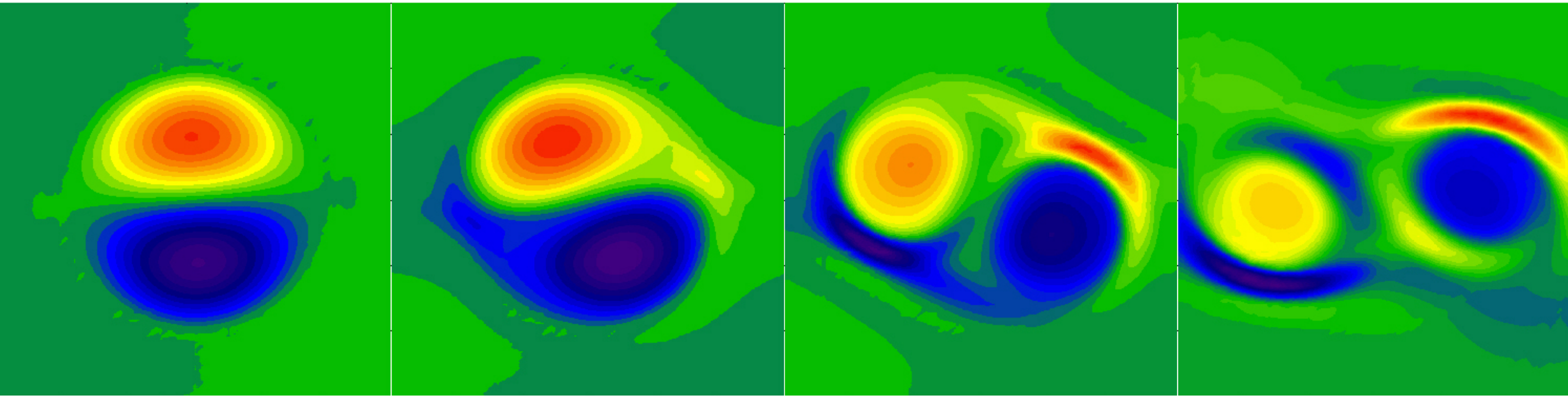

J: t=0.8 | J: t=3.2 | J: t=4.0 | J: t=4.8